Thermal Expansion Characteristics and Their Impact on Reinforced Concrete Bridges Under Varying Temperature Conditions

Jing Hu[1], JinKe Ji[1], Yanxiong Liu[2], Hao Cui[2], Peibo You[3*]

[1] Henan Transport Investment Jiaozheng Expressway Co., Ltd., Zhengzhou 450000, China
[2] Henan Province Highway Engineering Bureau Group Co., Ltd., Zhengzhou 450000, China
[3] Henan University of Urban Construction, Pingdingshan 467000, China

Corresponding Author Email: 30070513@huuc.edu.cn

ABSTRACT

Reinforced concrete bridges are a critical component of modern transportation infrastructure, but their performance is significantly affected by temperature variations. Fluctuations in environmental temperature lead to thermal expansion and contraction of materials, potentially posing challenges to the stability and safety of bridge structures. Existing studies primarily focus on the overall impact of temperature on bridge performance, providing valuable theoretical insights; however, most of these studies are based on simplified models that fail to comprehensively account for actual temperature fields and material heterogeneity. This limitation reduces the applicability of many research findings in practical scenarios. To address these gaps, this paper conducts an in-depth analysis of the thermal expansion characteristics of reinforced concrete bridges under varying temperature conditions. The study is divided into two main parts: the analysis of temperature fields in reinforced concrete bridges, and the analysis of thermal expansion characteristics under different temperature conditions, aiming to provide more accurate references for design and maintenance.

1. INTRODUCTION

In modern infrastructure construction, reinforced concrete bridges are widely used in various transportation projects due to their excellent mechanical properties and durability [1-5]. However, the long-term stability and safety of bridges are significantly affected by changes in environmental temperature [6, 7]. The effects of thermal expansion and contraction caused by temperature fluctuations have a profound impact on the structural integrity, functionality, and service life of bridges [8-11]. Particularly under extreme climatic conditions, the thermal expansion and contraction of bridge materials may cause cracks, deformation, and structural failure, which poses higher requirements for bridge maintenance and operation. Therefore, it is particularly important to conduct an in-depth study of the thermal expansion characteristics of reinforced concrete bridges under different temperature conditions.

Currently, research in related fields mainly focuses on the overall impact of temperature changes on bridges and the adjustment of design parameters [12-15]. These studies not only help engineers understand the behavior of materials under different temperature conditions but also provide important references for bridge design and maintenance. However, there are certain shortcomings in the existing research methods [16-20]. Many studies are still based on simplified theoretical models, which fail to fully consider the complex temperature distribution and material heterogeneity in actual engineering

projects [21, 23]. In addition, traditional research methods often lack dynamic monitoring and real-time analysis of the actual thermal expansion process of bridges, which may lead to deviations in the results when applied in practice [24, 25].

This paper aims to address the shortcomings of existing research by conducting an in-depth analysis of the thermal expansion characteristics of reinforced concrete bridges under different temperature conditions. The main content of the research includes two parts: first, the analysis of the temperature field of reinforced concrete bridges, and second, the analysis of the thermal expansion characteristics of bridges under different temperature conditions. Through precise measurements of the actual temperature field of bridges and systematic analysis of thermal expansion behavior, this paper will reveal the true thermal expansion characteristics of bridge materials under different temperature conditions and their impact on the structural performance of bridges. This research will provide more scientific evidence for bridge design, construction, and maintenance, thereby improving the safety and durability of bridges and contributing new theoretical support and practical guidance to the development of related engineering fields.

2. TEMPERATURE FIELD ANALYSIS OF REINFORCED CONCRETE BRIDGES

To accurately simulate the distribution of the temperature

field and heat transfer characteristics of reinforced concrete bridges, different types of heat transfer analysis elements were used. The DC3D8 three-dimensional heat transfer analysis element was selected for the concrete slab. DC3D8 is an eight-node linear heat transfer hexahedral element in ABAQUS used for thermal transfer analysis. Through this element, the temperature distribution along the thickness direction of the composite beam can be accurately obtained. The DC3D8 element is not constrained by space and can provide true and reliable temperature field simulation results, thereby providing the necessary data support for structural analysis. For the steel reinforcement mesh, the DC1D2 two-node heat transfer link element was used. This element is suitable for one-dimensional heat transfer analysis and can effectively simulate the heat transfer characteristics of the steel reinforcement mesh. In terms of mesh division, the grid size of the concrete flange is approximately 20×20×60 (mm)³. This division ensures the accuracy of the temperature field analysis while also considering computational efficiency. For the steel beam web and flange, two elements were divided in the thickness direction, with a grid size of 5×20×20 (mm)³ for the web and 6×20×20 (mm)³ for the flange. The grid size of the studs is 5.8 mm, and the grid size of the steel reinforcement mesh is 60 mm. Figure 1 shows the design diagram of the reinforced concrete bridge structure.

The internal heat transfer of a reinforced concrete bridge is mainly achieved through the process of heat conduction, that is, the transfer of heat between different materials and sections of the beam. Concrete and steel reinforcement have different thermal conductivities; therefore, they exhibit different heat conduction characteristics during temperature changes. By solving the sectional heat conduction equation, the variation of temperature with time and space can be simulated, thereby obtaining the temperature distribution within the bridge section.
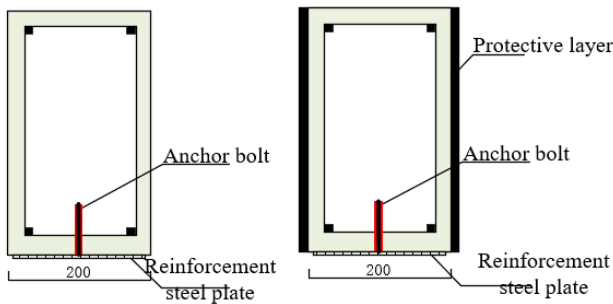
Figure 1. Design diagram of reinforced concrete bridge structure

The sectional heat conduction equation is usually derived from the basic equation of heat conduction, namely the Fourier heat conduction equation. This equation describes the heat transfer process within a material and expresses the relationship between thermal conductivity, temperature gradient, and heat flux. When constructing the sectional heat conduction equation, the bridge section is first decomposed into multiple discrete small elements, and the heat exchange between these small elements is considered. The equation includes parameters such as thermal conductivity, specific heat capacity, and material density, which determine the material's ability to transfer heat. In the solution process, numerical methods such as the finite difference method or the finite element method are usually used to discretize the

equation to calculate the temperature change of each small element. Assuming the sectional temperature of the reinforced concrete bridge is represented by S, the density of the reinforced concrete bridge material by ϑ, and the specific heat of the reinforced concrete bridge material by z, we have:

$$\frac{\partial S}{\partial s} = \frac{1}{z\vartheta}\left[\frac{\partial}{\partial a}\left(\eta\frac{\partial S}{\partial a}\right) + \frac{\partial}{\partial b}\left(\eta\frac{\partial S}{\partial b}\right) + \frac{\partial}{\partial c}\left(\eta\frac{\partial S}{\partial c}\right)\right] \quad (1)$$

The initial condition is set as the temperature of each node before the temperature rise, which serves as a starting reference point and provides a basis for subsequent analysis. The boundary conditions involve the heat exchange process between the outer surface of the bridge and the surrounding environment, including three main conditions. The initial boundary condition is:

$$S_{(a,b,c,s=0)} = S_0 = 20°C \quad (2)$$

The first type of boundary condition deals with the temperature of the fire-exposed surface of the reinforced concrete bridge as a function of time, which requires consideration of the variation of temperature over time to simulate the direct impact of the heat source on the bridge.

$$S_{(a,b,c,s)} = S(s) \quad (3)$$

The second type of boundary condition is the convective heat transfer boundary condition, which describes the convective heat exchange between the outer surface of the bridge and the surrounding air. This condition is used to simulate the effect of air flow on the heat transfer of the bridge surface. Assuming the convective heat transfer coefficient of the material is represented by α_1 and the boundary temperature of the reinforced concrete bridge by S_z, we have the formula:

$$\eta\frac{\partial S}{\partial a}m_a + \eta\frac{\partial S}{\partial b}m_b + \eta\frac{\partial S}{\partial c}m_c = -\alpha_1(S - S_z) \quad (4)$$

The third type of boundary condition involves thermal radiation, which considers the boundary heat flux generated by thermal radiation, reflecting the radiative transfer of surface temperature to the surrounding environment. Assuming the sectional shape factor of the reinforced concrete bridge is represented by θ, the emissivity of the reinforced concrete bridge material by γ_e, and the Stefan-Boltzmann constant by δ, we have the formula:

$$w_e = \theta\gamma_e\delta\left[(S - 273.15)^4 - (S_z - 273.15)^4\right] \quad (5)$$

3. ANALYSIS OF THERMAL EXPANSION CHARACTERISTICS OF REINFORCED CONCRETE BRIDGES UNDER DIFFERENT TEMPERATURE CONDITIONS

Under uniform heating conditions, all parts of a reinforced concrete bridge will undergo a synchronous temperature rise, leading to overall thermal expansion of the material. Due to the different coefficients of thermal expansion of steel and concrete, they will experience varying degrees of expansion

during the temperature rise. However, since the steel and concrete are tightly bonded in the bridge, their thermal expansions must be coordinated, forming a common axial thermal expansion. In this process, the axial temperature strain of the bridge is a key indicator for measuring this expansion behavior. As the temperature increases, the various components of the bridge gradually expand, and the axial strain increases accordingly. For ideal uniform heating conditions, the axial temperature strain will change linearly, meaning that the strain value is proportional to the extent of the temperature increase. This linear relationship is primarily determined by the thermal expansion coefficient of the bridge materials. As the temperature continues to rise, the thermal stress within the material will also increase. At this point, if the bridge's boundary conditions do not change, the axial thermal expansion strain will continue to increase until it reaches the material's thermal expansion limit. If the bridge is restricted by external constraints, such as abutments or supports, thermal expansion will be inhibited, resulting in additional stress within the structure, which may lead to cracks or other damage. Therefore, a detailed analysis of the thermal expansion characteristics of bridges under different temperature conditions is crucial to ensuring their structural safety and long-term durability. Figure 2 shows the layout of the temperature measurement points in the cross-section of the reinforced concrete bridge. Assuming the coefficient of thermal expansion of the material is represented by β, and the temperature change of the beam under uniform heating is represented by ΔS, the formula for calculating the thermal expansion temperature strain γ_S is given by:

$$\gamma_S = \beta \Delta S \qquad (6)$$

(a) With protective layer

(b) Without protective layer
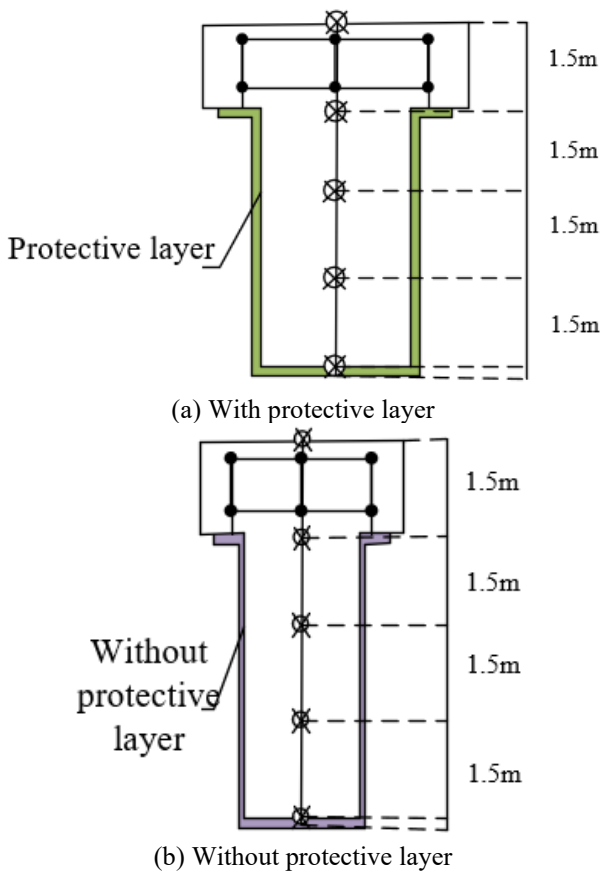
Figure 2. Layout of temperature measurement points in cross-section of reinforced concrete bridge

3.1 Axial deformation of unconstrained bridges

Under uniform heating conditions, an unconstrained reinforced concrete bridge will experience axial expansion elongation. The main influencing factors include the thermal expansion coefficient of the material, the initial size of the bridge, and the extent of the temperature change. The different thermal expansion coefficients of steel and concrete lead to different degrees of expansion during the heating process, thus affecting the overall expansion behavior. The thermal expansion coefficient of concrete is usually larger, resulting in a significantly greater expansion of the concrete part under the same temperature rise conditions compared to the steel. This difference leads to significant axial elongation of the entire bridge under unconstrained conditions. When calculating the expansion elongation of the bridge, the strain caused by temperature changes must first be considered, which is usually given by the product of the thermal expansion coefficient and the extent of the temperature rise. The calculation span M of the bridge, i.e., the length of the bridge span, is also an important parameter for calculating the expansion elongation because it directly affects the overall expansion amount caused by temperature changes. A larger span means a greater absolute amount of expansion under the same temperature rise. The calculation formula is given by:

$$\Delta M = M\gamma_S = M\beta \Delta S \qquad (7)$$

For statically determinate bridges, under uniform heating conditions, the reason why the bridge should be in a zero-stress state is related to its design and material characteristics. When the bridge is in a zero-stress state, its total strain is entirely composed of thermal expansion strain, and there is no additional internal force. The design of statically determinate bridges ensures that the stress within the bridge structure can be balanced under thermal expansion, thereby avoiding excessive internal stress caused by structural constraints. In this state, the total strain of the bridge equals the thermal expansion temperature strain because all deformation originates from thermal expansion rather than structural constraints or external loads. Specifically, thermal expansion strain is determined by the thermal expansion coefficients of steel and concrete and the extent of the temperature change as the temperature rises. When the bridge is uniformly heated and not constrained, its internal stress can remain balanced within the design range, allowing the total strain to be entirely composed of thermal expansion temperature strain, which is:

$$\gamma_{TO} = \gamma_{TH} \qquad (8)$$

3.2 Axial deformation of fully constrained bridges

For a fully constrained support bridge with axial deformation, the thermal expansion axial deformation caused by uniform heating is fully constrained at the support points, resulting in thermal expansion temperature reaction force O opposite to the direction of expansion at these support points. This reaction force is similar to the force on a compression member, with its magnitude and direction opposite to the axial deformation caused by thermal expansion of the bridge. The main factors influencing the thermal expansion temperature reaction force include the material's elastic modulus and the cross-sectional area of the bridge. The larger the elastic

modulus R of the material, the stronger the bridge's ability to respond to strain caused by thermal expansion, thus generating a greater reaction force. Furthermore, the larger the cross-sectional area of the bridge, the more significant the effect of the reaction force, as the reaction force O is proportional to the cross-sectional area X. In specific calculations, the thermal expansion strain γS needs to be calculated based on the actual temperature increase ΔS of the bridge and the thermal expansion coefficient β of the material, and then the reaction strain γ_l is determined through the equilibrium equation. In the absence of additional loads, the thermal expansion strain γ_S and the reaction strain γ_l are equal in magnitude and opposite in direction, i.e., $\gamma_S = -\gamma_l$. Then, O is given by:

$$O = R\gamma_l X = -R\gamma_S X = -RX\beta\Delta S \qquad (9)$$

In a fully constrained support bridge with axial deformation, as the temperature increase ΔS rises, the thermal expansion temperature reaction force O will gradually increase. When the reaction force generated by thermal expansion reaches a certain level, it may lead to bridge failure. The failure modes of the bridge are similar to those of a compression member, mainly including material strength failure, stability failure, and a combination of these two modes. Material strength failure usually occurs when the stress caused by the reaction force exceeds the material's yield strength, causing the material to yield and lose its load-bearing capacity. Stability failure occurs when the slenderness ratio of the bridge is large; as the reaction force increases, the bridge may buckle and lose overall stability.

Specifically, for members with a small slenderness ratio, material yielding typically occurs before buckling. As the temperature rises, the axial pressure generated by thermal expansion gradually increases, and once the yield strength of the material is reached, the member will enter an elastic-plastic phase. In this case, although the stress remains at the yield strength level, the plastic strain of the material will continue to increase, leading to excessive deformation and potential failure of the member under prolonged high temperatures. Assuming the material's flexural elastic modulus of the cross-section at temperature S is represented by $R(S)$, the yield strength of the material is represented by δ_b, and the material's thermal expansion coefficient is represented by β, temperature ΔS that causes material yielding can be calculated by:

$$\Delta S_b = \frac{\delta_b}{R(S)\beta} \qquad (10)$$

For members with a large slenderness ratio, they will buckle before the material yields. When the temperature continues to rise until the member reaches the critical buckling force O_{ze}, assuming the material is still elastic and its properties do not change with temperature, the temperature reaction force O will remain unchanged. However, due to the increase in temperature strain, the member will undergo greater deformation, potentially leading to further buckling or stability problems. Therefore, members with a large slenderness ratio are more likely to experience instability under high-temperature conditions, especially when deformation cannot be effectively controlled through design measures. Assuming the calculation length of the member is represented by m, O_{ze} is calculated by:

$$O_{ze} = \frac{\tau^2 R(S)m}{m^2} \qquad (11)$$

Under the action of temperature S, let $O_{ze} = O$, and combining the above equation with Eq. (9), we get:

$$R(S)X\beta\Delta S = \frac{\tau^2 R(S)U}{m^2} \qquad (12)$$

Assuming the slenderness ratio of the member is represented by $\eta = m/e$, and the radius of gyration of the cross-section is represented by e, the critical buckling temperature increment is obtained by:

$$\Delta S_{ze} = \frac{\tau^2}{\beta}\left(\frac{e}{m}\right)^2 = \frac{\tau^2}{\beta\eta^2} \qquad (13)$$

Based on research findings, the response of members to temperature loads shows significant differences in the elastic and elastic-plastic phases. For simply supported members, as the temperature rises, the mid-span deformation increases, and this deformation is related to the slenderness ratio of the member—when the slenderness ratio increases, the deformation decreases. This indicates that the slenderness ratio has a significant impact on the deformation caused by temperature, with members with a large slenderness ratio exhibiting relatively small deformations, demonstrating better stability. For slender elastic members under constraints, in terms of changes in axial force, deformation, and bending moment with increasing temperature, the axial force tends to be constant beyond 150°C, indicating that thermal expansion mainly manifests in the form of deformation rather than increasing axial force. This characteristic helps prevent structural damage caused by stress from thermal expansion, especially in terms of the safety of connection nodes. Meanwhile, the increase in axial force and bending moment caused by temperature can effectively counteract the bending moment caused by uniform loads, enhancing the fire resistance of members under high-temperature conditions. In terms of the axial force and deformation of mid-span sections of ideal elastic-plastic material members with temperature changes, elastic-plastic members show nonlinear stress and deformation behavior at high temperatures, which differs from the behavior of elastic members under high temperatures.

3.3 Axial deformation with incomplete constraint

In practical engineering, fully constrained members are not realistic during thermal expansion, so constraints on axial deformation due to thermal expansion are usually simulated by assuming springs with infinite stiffness. In the case of incomplete axial deformation constraints, the thermal expansion temperature stress and critical buckling temperature changes of reinforced concrete bridges are affected by multiple factors. Thermal expansion temperature stress is mainly influenced by the thermal expansion coefficient of the bridge material, the elastic modulus, and the actual constraint conditions. Specifically, as the temperature rises, the thermal expansion of steel and concrete will cause temperature stress within the bridge, which is generally directly related to the material's thermal expansion coefficient β and the temperature increase ΔS. The elastic modulus R of the material and the

stiffness of the structure will also affect the magnitude of the stress. For the variation of the critical buckling temperature, the influencing factors include the slenderness ratio of the member, the elastic modulus of the material, and the geometric characteristics of the member. In the case of incomplete axial deformation constraints, an increase in the slenderness ratio of the member will generally reduce its critical buckling temperature. To estimate the critical buckling temperature, the Euler buckling formula from stability analysis can be used, which involves the geometric parameters and material properties of the member. When the temperature continues to rise and approaches or exceeds the critical buckling temperature, the member will undergo buckling failure. Thermal expansion temperature stress can be calculated by:

$$\delta = \frac{R\beta\Delta S}{1 + RX/j_s M} \qquad (14)$$

The change in critical buckling temperature can be calculated by:

$$\Delta S_{ze} = \frac{\tau^2}{\beta\eta^2}\left(1 + \frac{RX}{j_s M}\right) \qquad (15)$$

Based on the ratio of spring stiffness j_s to the axial deformation stiffness RX/M of the member, slender members may buckle when the temperature is not high. In this case, the end restraint of the member has little effect on the buckling critical temperature because the large slenderness ratio of the member makes its primary buckling behavior less affected by the end restraint stiffness. However, when the slenderness ratio is less than about 100, the stiffness of the end restraint of the member significantly affects the buckling critical temperature. This is because the stiffness of the end restraint directly affects the overall stability of shorter members in fire conditions. The stronger the end restraint, the higher the buckling critical temperature of the member under high-temperature conditions, thereby reducing the risk of buckling failure. For reinforced concrete bridges, the axial deformation caused by thermal expansion under fire conditions increases internal stress, and the end restraint stiffness of the member can be optimized through design and construction measures to improve the stability of the bridge at high temperatures. When members with a small slenderness ratio are exposed to high temperatures, if the end restraint stiffness is insufficient, buckling may occur at lower temperatures, leading to bridge failure. Figure 3 shows the reinforced concrete bridge specimens model 1 and model 2 used in the test.
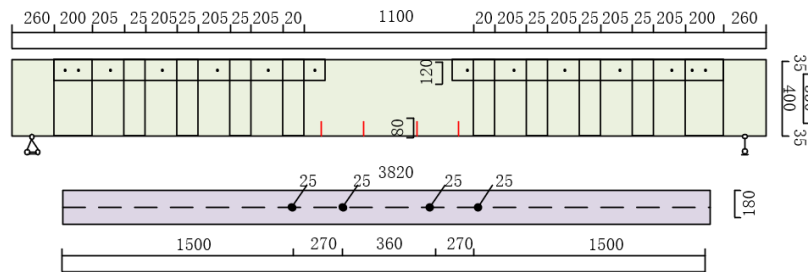

Figure 3. Reinforced concrete bridge specimens model 1 and model 2

4. EXPERIMENTAL RESULTS AND ANALYSIS

Tables 1, 2, and 3 respectively provide an introduction to the finite element model parameters of reinforced concrete bridges. Based on the experimental data analysis in Figure 4, it can be observed that under different temperature conditions, the mid-span vertical deflection of bridge models 1-1 and 1-2, as well as models 2-1 and 2-2, gradually increases over time. In Figure 4-1, the mid-span vertical deflection of model 1-1 and model 1-2 shows a gradual difference after 40 minutes during the temperature rise. Especially at 120 minutes, the mid-span vertical deflection of model 1-2 reaches 60, while that of model 1-1 is 57.5. The data in Figure 4-2 further shows that the mid-span vertical deflection of models 2-1 and 2-2 also exhibits different growth trends throughout the experiment. At 240 minutes, the mid-span vertical deflection of model 2-1 is 42.3, while that of model 2-2 is 39.6. These data indicate that the choice of different models and material standards has a significant impact on the thermal expansion characteristics of bridges. From the experimental results, it can be concluded that the thermal expansion characteristics of reinforced concrete bridges under different temperature conditions are influenced by multiple factors, including the constitutive relationship of steel and concrete, the thermal expansion coefficient, and the choice of material standards. In

particular, when different material standards (such as EN1993-1-2 and ASCE) are used, the thermal expansion behavior of the bridge changes significantly. Models 1-2 and 2-2 adopt the ASCE standard for the steel thermal expansion coefficient, resulting in a larger expansion coefficient under high-temperature conditions, indicating that steel under the ASCE standard is more prone to expansion at high temperatures.

By analyzing the data in Table 2 and Figure 5, it can be seen that there are significant differences in the thermal expansion characteristics of reinforced concrete bridges under different models. In Figure 5-1, the mid-span vertical deflection of model 1-1 and model 1-3 shows different growth trends as time increases. Particularly for model 1-3, when the time reaches 140, its mid-span vertical deflection is significantly higher than that of model 1-1, reaching 134, while model 1-1 is only 90. In Figure 5-2, the mid-span vertical deflection of model 2-3 also significantly exceeds that of model 2-1 as time increases, with model 2-3 having a coefficient of 54 and model 2-1 having a coefficient of 44.1 at 240 minutes. These results indicate that different finite element models and material constitutive relationships have a significant impact on the thermal expansion behavior of bridge structures. Data analysis shows that the thermal expansion coefficients of the concrete and steel used in the model, as well as the material constitutive relationships, play a key role in the thermal expansion

characteristics of the bridge. In model 1-3 and model 2-3, due to the use of the EN1992-1-2 standard for the concrete thermal expansion coefficient, the thermal expansion behavior of the reinforcement is more pronounced, which may lead to greater expansion and stress concentration of the bridge under high-temperature conditions. In contrast, the ASCE standard thermal expansion coefficients used in models 1-1 and 2-1 show relatively smaller expansion coefficients, suggesting that their design may be more suitable for environments with large temperature variations.

Table 1. Introduction to finite element model parameters (Thermal Expansion Coefficient of Bridge Reinforcement)

Model	Concrete Constitutive Relationship	Concrete Expansion Angle	Concrete Thermal Expansion Coefficient	Steel Constitutive Relationship	Steel Thermal Expansion Coefficient
model 1-1	EN1992-1-2	38°	ASCE	Elastic-Plastic	EN1993-1-2
model 1-2	EN1992-1-2	38°	ASCE	Elastic-Plastic	ASCE
model 2-1	EN1992-1-2	38°	ASCE	Elastic-Plastic	EN1993-1-2
model 2-2	EN1992-1-2	38°	ASCE	Elastic-Plastic	ASCE

Table 2. Introduction to finite element model parameters (Thermal Expansion Coefficient of Bridge Concrete)

Model	Concrete Constitutive Relationship	Concrete Expansion Angle	Concrete Thermal Expansion Coefficient	Steel Constitutive Relationship	Steel Thermal Expansion Coefficient
model 1-1	EN1992-1-2	38°	ASCE	Elastic-Plastic	EN1993-1-2
model 1-3	EN1992-1-2	38°	EN1992-1-2	Elastic-Plastic	EN1993-1-2
model 2-1	EN1992-1-2	38°	ASCE	Elastic-Plastic	EN1993-1-2
model 2-3	EN1992-1-2	38°	EN1992-1-2	Elastic-Plastic	EN1993-1-2

(1) *model* 1   (2) *model* 2
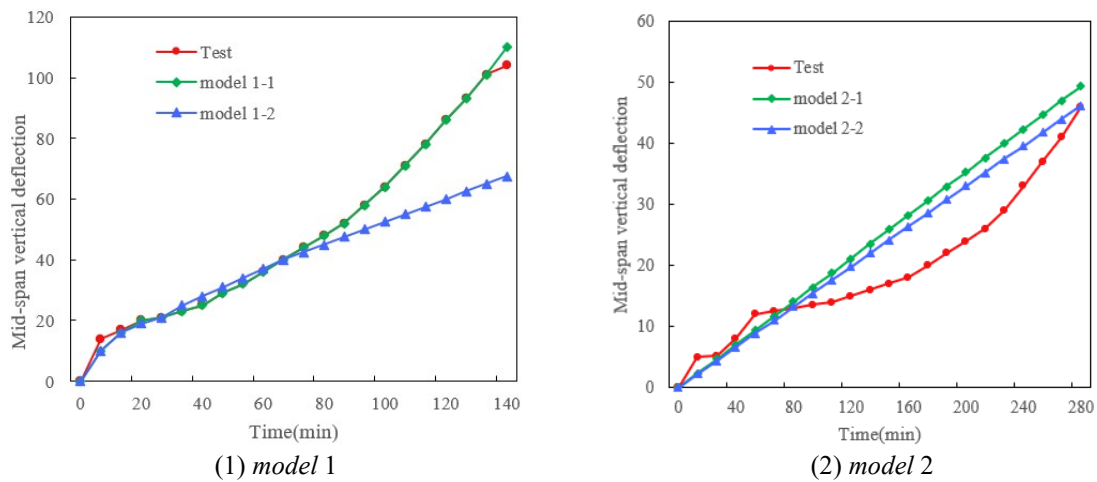
Figure 4. Comparative analysis of thermal expansion coefficients of bridge reinforcement

Table 3. Introduction to finite element model parameters (Concrete Expansion Angle of Bridge)

Model	Concrete Constitutive Relationship	Concrete Expansion Angle	Concrete Thermal Expansion Coefficient	Steel Constitutive Relationship	Steel Thermal Expansion Coefficient
model 1-1	EN1992-1-2	38°	ASCE	Elastic-Plastic	EN1993-1-2
model 1-4	EN1992-1-2	40°	ASCE	Elastic-Plastic	EN1993-1-2
model 1-5	EN1992-1-2	42°	ASCE	Elastic-Plastic	EN1993-1-2
model 2-1	EN1992-1-2	38°	ASCE	Elastic-Plastic	EN1993-1-2
model 2-4	EN1992-1-2	40°	ASCE	Elastic-Plastic	EN1993-1-2
model 2-5	EN1992-1-2	42°	ASCE	Elastic-Plastic	EN1993-1-2

(1) *model* 1   (2) *model* 2
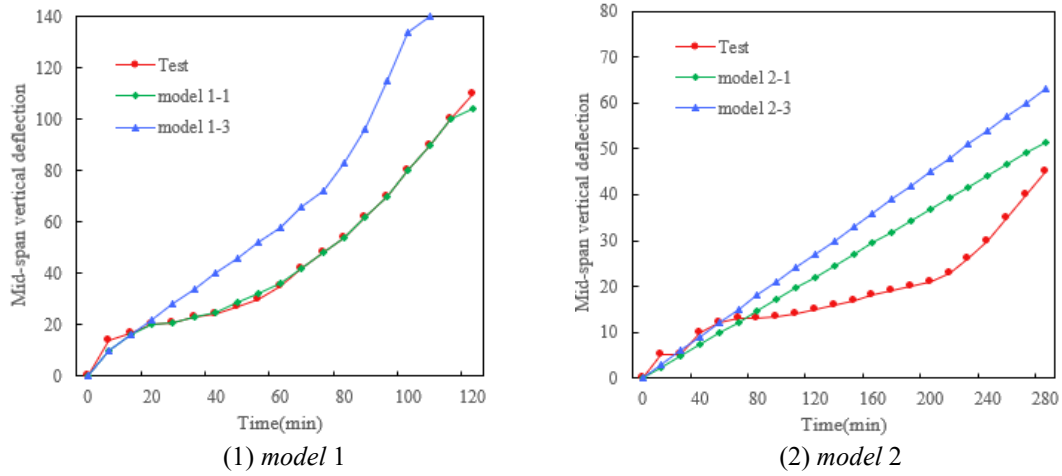
Figure 5. Comparative analysis of thermal expansion coefficients of bridge concrete

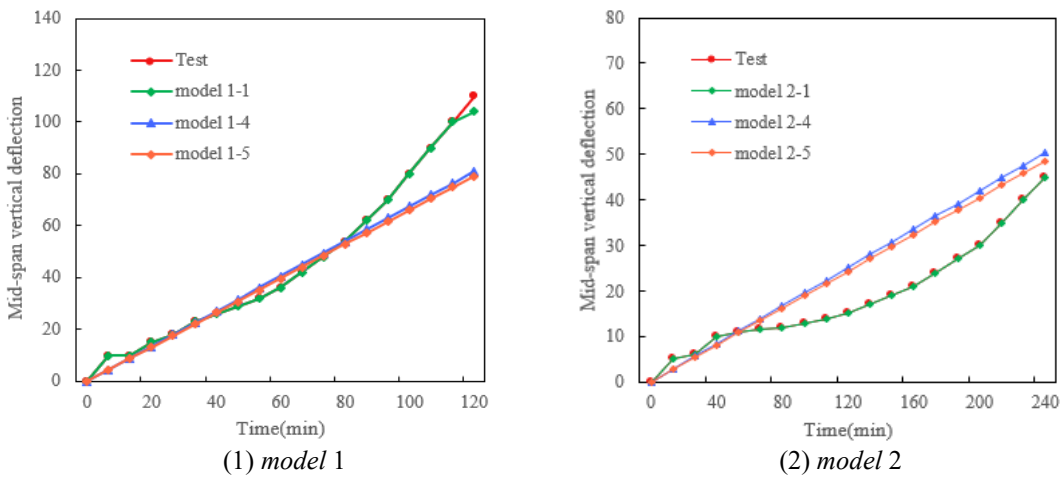(1) *model* 1   (2) *model* 2

Figure 6. Comparative analysis of concrete expansion angles of bridges

According to the data analysis in Table 3 and Figure 6-1, the changes in the thermal expansion coefficients of reinforcement in bridge models 1-1 and 1-4 at different time points show the significant impact of concrete expansion angle on thermal expansion behavior. The expansion coefficient of model 1-1 at 60 minutes is 15, while for model 1-4 at the same time point it is 17, demonstrating that model 1-4 has a stronger thermal expansion capability at a higher expansion angle. As the test time extends, the expansion coefficient of model 1-4 continues to be higher than that of model 1-1, reaching 29 at 120 minutes, while model 1-1 is 26. This indicates that an increase in the concrete expansion angle can significantly enhance the thermal expansion coefficient of reinforcement. Figure 6-2 shows the variation in thermal expansion coefficients of reinforcement in models 2-1, 2-4, and 2-5 with time under different concrete expansion angles. The data shows that as the concrete expansion angle increases (from 38° to 42°), the thermal expansion coefficient of reinforcement also increases. For example, at the 240-time point, the thermal expansion coefficient of reinforcement for model 2-1 is 45, while those for models 2-4 and 2-5 are 50.4 and 48.6, respectively. It can be seen that the increase in the expansion angle causes an overall increase in the thermal expansion coefficient of reinforcement, especially with a more significant increase at higher time points. The data indicates that the increase in the concrete expansion angle has a noticeable effect on the thermal expansion coefficient of

reinforcement. A larger expansion angle (e.g., 42°) leads to more pronounced thermal expansion of the reinforcement, possibly due to the enhanced additional restraint force of the concrete on the reinforcement, which intensifies the strain of the reinforcement under temperature changes. This effect is particularly prominent under prolonged heating conditions.
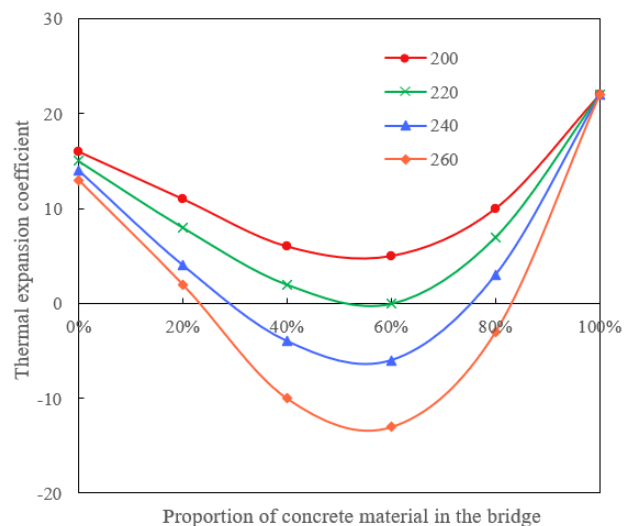

Figure 7. Impact of protrusion length and concrete material proportion on bridge thermal expansion

According to the data provided in Figure 7, the protrusion length of reinforced concrete bridges shows a significant variation under different slenderness ratios of concrete material (ranging from 0% to 100%). For example, when the concrete material proportion is 20%, the protrusion length is 16 mm at 200 mm, 8 mm at 220 mm, and 4 mm and 2 mm at 240 mm and 260 mm, respectively. As the concrete material proportion increases, the protrusion length gradually decreases, especially when the material proportion reaches 40%, where the protrusion length becomes negative, indicating a significant contraction phenomenon. When the concrete material proportion reaches 100%, regardless of the protrusion length, it stabilizes at 22 mm, showing the ultimate expansion effect of the material. This indicates that the slenderness ratio of concrete material has a significant impact on the thermal expansion characteristics of the bridge. From the data analysis, it can be concluded that the proportion of concrete material has a significant effect on the thermal expansion behavior of reinforced concrete bridges. As the concrete material proportion increases, the protrusion length gradually decreases, especially when the proportion reaches 40%, showing a significant contraction phenomenon. This phenomenon may be due to the shrinkage effect of concrete at high temperatures surpassing its expansion effect. For high-proportion concrete materials (e.g., 100%), the protrusion length of the bridge stabilizes at a higher value, indicating that under these conditions, the expansion effect of concrete dominates.
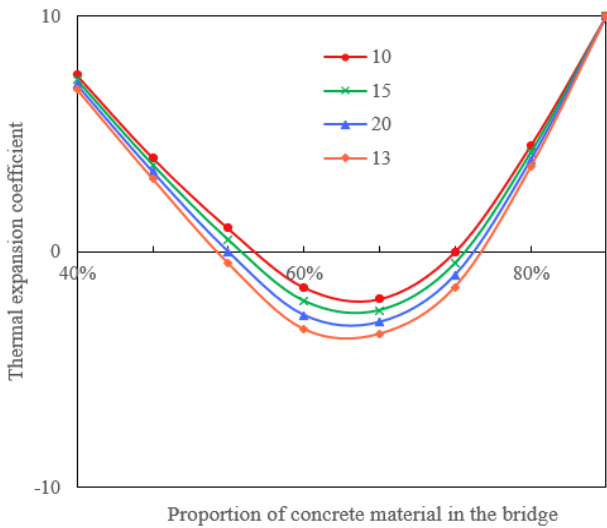
Figure 8. Impact of slenderness ratio and concrete material proportion on bridge thermal expansion

From the data in Figure 8, it can be observed that the slenderness ratio of the bridge under different concrete material proportions has a significant impact on the thermal expansion behavior. When the concrete material proportion is 40%, the slenderness ratio decreases from 10 to -1.5, showing that the expansion effect of the material decreases with increasing proportion. When the proportion is 60% and 80%, the slenderness ratio continues to decrease to -2 and -1, further indicating a contraction phenomenon of the material. These changes show a certain pattern under different slenderness ratios; for example, the range of change is the smallest when the slenderness ratio is 15, while at a slenderness ratio of 20, the contraction effect is the most pronounced. Overall, as the concrete material proportion increases, the thermal expansion effect gradually weakens, manifested as an increase in the

negative value of the slenderness ratio. Data analysis shows that the proportion of concrete material has a significant impact on the thermal expansion characteristics of the bridge. Specifically, an increase in the proportion of concrete material leads to a decrease in the slenderness ratio, thereby reflecting an enhanced contraction effect of the material. This phenomenon indicates that at a higher concrete proportion, the thermal expansion capacity of the bridge material is inhibited, leading to a weakening of its overall thermal expansion performance.
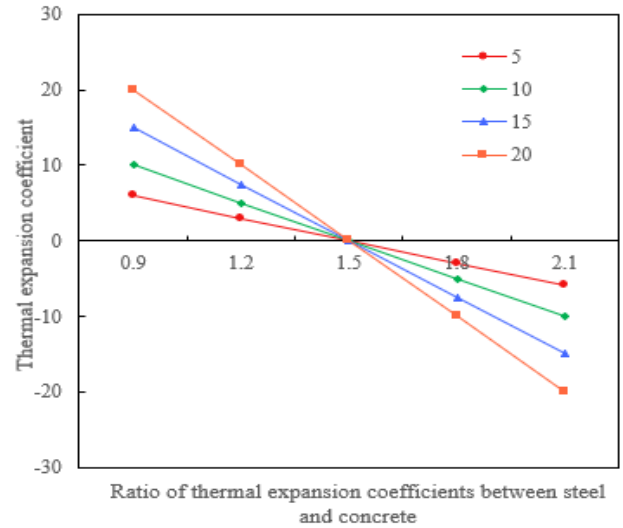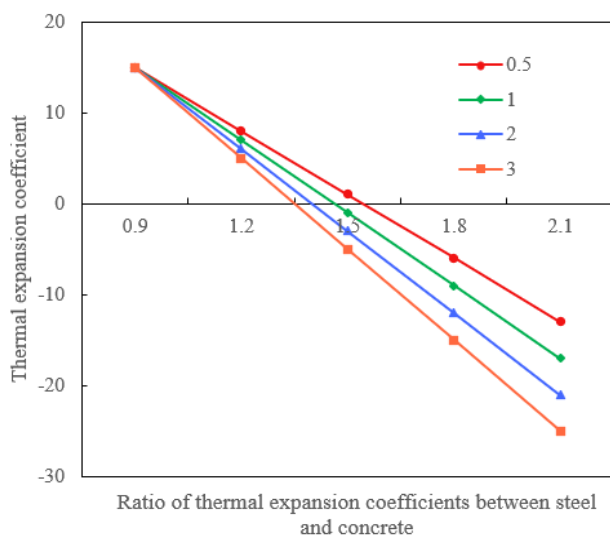

Figure 9. Impact of the difference in thermal expansion coefficients between steel and concrete, and the concrete thermal expansion coefficient on bridge thermal expansion

From the data in Figure 9, it can be seen that the ratio of the thermal expansion coefficient between steel and concrete and the concrete thermal expansion coefficient has a significant impact on the thermal expansion characteristics of the bridge. Specifically, when the ratio of the thermal expansion coefficient between steel and concrete is 0.9, the concrete thermal expansion coefficient is 5, and the difference is -6; when the ratio increases to 1.2, the concrete thermal expansion coefficient is 10, and the difference is -10; further increasing the ratio to 2.1, the concrete thermal expansion coefficient is 20, and the difference is -20. This shows that as the ratio of the thermal expansion coefficient between steel and concrete increases, the difference in the concrete thermal expansion coefficient gradually expands, showing a linear increasing trend. Data analysis indicates that an increase in the ratio of the thermal expansion coefficient between steel and concrete significantly affects the thermal expansion behavior of concrete. Specifically, when the ratio of the thermal expansion coefficient between steel and concrete increases, the difference in the concrete thermal expansion coefficient shows a noticeable increasing trend. This suggests that when designing bridges, the thermal expansion properties of steel and concrete materials should be fully considered to ensure the stability and safety of the structure under different temperature conditions.

The data from Figure 10 indicates that changes in the ratio of the thermal expansion coefficient between steel and concrete have a significant impact on the slenderness ratio of the bridge. When the ratio of the thermal expansion coefficient between steel and concrete increases from 0.9 to 2.1, the slenderness ratio shows a significant downward trend under

different thermal expansion coefficients. For example, when the ratio of the thermal expansion coefficient between steel and concrete is 0.9, the slenderness ratio is 15; when the ratio increases to 2.1, the slenderness ratio decreases to -13. This change shows a decreasing trend under different ratios of the thermal expansion coefficient between steel and concrete, especially when the difference in the thermal expansion coefficient increases, the negative value of the slenderness ratio increases significantly. This indicates that the difference in thermal expansion coefficients has a direct impact on the expansion behavior of bridge materials. From the data analysis, it can be seen that the ratio of the thermal expansion coefficient between steel and concrete has an important impact on the thermal expansion characteristics of the bridge. As the ratio of the thermal expansion coefficient between steel and concrete increases, the negative value of the slenderness ratio increases, indicating that the difference in thermal expansion coefficients intensifies the contraction effect of the material. Especially at higher coefficient ratios, the slenderness ratio decreases significantly, indicating that the unevenness of material expansion under high-temperature conditions is enhanced. Therefore, in the bridge design process, the thermal expansion properties of steel and concrete should be comprehensively considered to optimize the structural stability and durability of the bridge.

Figure 10. impact of concrete material proportion and the difference in thermal expansion coefficients between steel and concrete on bridge thermal expansion

5. CONCLUSION

This paper conducted an in-depth analysis of the thermal expansion characteristics of reinforced concrete bridges under different temperature conditions, mainly covering two aspects: temperature field analysis and bridge thermal expansion characteristics analysis. The study includes the comparison of the thermal expansion coefficients of steel and concrete, the impact of the concrete expansion angle, the effect of protrusion length and concrete material proportion on bridge thermal expansion, the influence of slenderness ratio on bridge thermal expansion, the impact of the difference in thermal expansion coefficients between steel and concrete on bridge thermal expansion, and the combined effect of concrete material proportion and the difference in thermal expansion

coefficients. The experimental results show that the concrete expansion angle, the thermal expansion coefficients of steel and concrete, and the material proportion have a significant impact on the thermal expansion characteristics of the bridge, especially under high-temperature conditions, where the expansion behavior of materials is more pronounced, affecting the overall structural performance of the bridge.

The research in this paper reveals the thermal expansion characteristics of steel and concrete under different temperature conditions and their impact on the bridge structure. The study shows that the concrete expansion angle and material proportion significantly affect the thermal expansion characteristics of the bridge, especially in cases of prolonged heating, where this effect is particularly evident. These findings provide important references for bridge design and material selection, helping to optimize the heat resistance and structural stability of bridges. However, there are certain limitations to this study, such as the actual performance under different environmental conditions still needing further verification. In addition, future research can further explore the thermal expansion characteristics of different types of bridges and complex environments to provide more comprehensive design guidance and optimization recommendations.

REFERENCES

[1] Sun, L., Zhou, Y., Min, Z. (2018). Experimental study on the effect of temperature on modal frequencies of bridges. International Journal of Structural Stability and Dynamics, 18(12): 1850155. https://doi.org/10.1142/S0219455418501559

[2] Krkoska, L., Moravcik, M. (2017). Monitoring of temperature gradient development of highway concrete bridge. In MATEC Web of Conferences, 117: 00091. https://doi.org/10.1051/matecconf/201711700091

[3] Cho, K., Cho, J.R. (2022). Effect of temperature on the modal variability in short-span concrete bridges. Applied Sciences, 12(19): 9757. https://doi.org/10.3390/app12199757

[4] Gao, L., Qian, J., Ding, X., Guan, M., Liao, M., Xu, Z. (2023). Experimental study for temperature variation of bridge pier in plateau area using optical frequency domain reflectometer technology. IEEE Sensors Journal, 23(6): 5810-5817. https://doi.org/10.1109/JSEN.2023.3240314

[5] Zhang, L. M., Chao, W.W., Liu, Z.Y., Cong, Y., Wang, Z.Q. (2022). Crack propagation characteristics during progressive failure of circular tunnels and the early warning thereof based on multi-sensor data fusion. Geomechanics and Geophysics for Geo-Energy and Geo-Resources, 8: 172. https://doi.org/10.1007/s40948-022-00482-3

[6] Liu, H., Wu, S., Zhang, Y., Hu, T. (2023). Finite element simulation of temperature variations in concrete bridge girders. Fluid Dynamics & Materials Processing, 19(6): 1551. https://doi.org/10.32604/fdmp.2023.024430

[7] Wang, D., Tan, B., Wang, X., Zhang, Z. (2021). Experimental study and numerical simulation of temperature gradient effect for steel-concrete composite bridge deck. Measurement and Control, 54(5-6): 681-691. https://doi.org/10.1177/00202940211007166

[8] Kuryłowicz-Cudowska, A. (2019). Determination of

thermophysical parameters involved in the numerical model to predict the temperature field of cast-in-place concrete bridge deck. Materials, 12(19): 3089. https://doi.org/10.3390/ma12193089

[9] Nguyen, V.H. (2024). An investigation of cracks caused by concrete shrinkage and temperature difference in common reinforced concrete bridge structures. Frattura ed Integrità Strutturale, 18(68): 242-254. https://doi.org/10.3221/IGF-ESIS.68.16

[10] Elshoura, A., Okeil, A.M. (2024). Simplified method for estimating restraint moment induced by vertical temperature gradient in continuous prestressed concrete bridges and verification using AASHTO BDS. Structure and Infrastructure Engineering, 20(6): 944-956. https://doi.org/10.1080/15732479.2022.2132518

[11] Krkoška, L., Moravčík, M. (2016). The measurement of thermal changes on concrete box girder bridge. In MATEC Web of Conferences, 86: 01003. https://doi.org/10.1051/matecconf/20168601003

[12] Hagedorn, R., Martí-Vargas, J.R., Dang, C.N., Hale, W. M., Floyd, R.W. (2019). Temperature gradients in bridge concrete I-girders under heat wave. Journal of Bridge Engineering, 24(8): 04019077. https://doi.org/10.1061/(ASCE)BE.1943-5592.0001454

[13] Fan, J.S., Li, B.L., Liu, C., Liu, Y.F. (2022). An efficient model for simulation of temperature field of steel-concrete composite beam bridges. In Structures, 43: 1868-1880. https://doi.org/10.1016/j.istruc.2022.05.079

[14] Tian, Y., Zhang, N., Xia, H. (2017). Temperature effect on service performance of high-speed railway concrete bridges. Advances in structural engineering, 20(6): 865-883. https://doi.org/10.1177/1369433216665306

[15] Hossain, T., Segura, S., Okeil, A.M. (2020). Structural effects of temperature gradient on a continuous prestressed concrete girder bridge: Analysis and field measurements. Structure and Infrastructure Engineering, 16(11): 1539-1550. https://doi.org/10.1080/15732479.2020.1713167

[16] Markova, J. (2018). models of thermal actions for steel and composite bridges based on monitoring. In IOP Conference Series: Materials Science and Engineering, 419(1): 012041. https://doi.org/10.1088/1757-899X/419/1/012041

[17] Abid, S.R., Tayşi, N., Özakça, M. (2016). Experimental analysis of temperature gradients in concrete box-girders. Construction and Building Materials, 106: 523-532. https://doi.org/10.1016/j.conbuildmat.2015.12.144

[18] Abaza, H., Shenawa, A., Semmelink, S. (2023). Using radiant heating system to prevent bridge freezing. In Heat Transfer Summer Conference, 87165: V001T12A001. https://doi.org/10.1115/HT2023-105739

[19] He, W.Y., Li, Z., Zhou, L., Ren, W.X., Li, Y. (2023). The effect of environmental temperature on influence line of concrete beam type bridge. In Structures, 48: 1468-1478. https://doi.org/10.1016/j.istruc.2023.01.058

[20] Bajzecerová, V., Kanócz, J. (2016). The effect of environment on timber-concrete composite bridge deck. Procedia engineering, 156: 32-39. https://doi.org/10.1016/j.proeng.2016.08.264

[21] Zhang, L. M., Cong, Y., Meng, F. Z., Wang, Z. Q., Zhang, P., Gao, S. (2021). Energy evolution analysis and failure criteria for rock under different stress paths. Acta Geotechnica, 16(2): 569-580. https://doi.org/10.1007/s11440-020-01028-1

[22] OBrien, E.J., Heitner, B., Žnidarič, A., Schoefs, F., Causse, G., Yalamas, T. (2020). Validation of bridge health monitoring system using temperature as a proxy for damage. Structural Control and Health Monitoring, 27(9): e2588. https://doi.org/10.1002/stc.2588

[23] Abid, S.R., Abbass, A.A., Alhatmey, I.A. (2019). Seasonal temperature gradient distributions in concrete bridge girders: A finite element study. In 2019 12th International Conference on Developments in eSystems Engineering (DeSE), Kazan, Russia, pp. 374-379. https://doi.org/10.1109/DeSE.2019.00075

[24] Semendary, A.A., Steinberg, E.P., Walsh, K.K., Barnard, E. (2019). Effects of temperature distributions on thermally induced behavior of UHPC shear key connections of an adjacent precast prestressed concrete box beam bridge. Journal of Bridge Engineering, 24(2): 04018115. https://doi.org/10.1061/(ASCE)BE.1943-5592.000134

[25] Kuryłowicz-Cudowska, A., Wilde, K., Chróścielewski, J. (2020). Prediction of cast-in-place concrete strength of the extradosed bridge deck based on temperature monitoring and numerical simulations. Construction and Building Materials, 254: 119224. https://doi.org/10.1016/j.conbuildmat.2020.119224